Solution of Some One- and Two-Dimensional Master Equation Models for Thermal Dissociation: The Dissociation of Methane in the Low-Pressure Limit

James A. Miller* and Stephen J. Klippenstein*

Combustion Research Facility, Sandia National Laboratories, Livermore, California 94551-0969

Christophe Raffy

Institut National Polytechnique de Grenoble, Grenoble, France

Received: December 10, 2001; In Final Form: February 25, 2002

Using three formulations of the master equation (ME), we have investigated theoretically the dissociation of methane in the low-pressure limit. The three forms of the ME are as follows: (1) A one-dimensional model in which E, the total energy, is the independent variable (the E model). (2) The two-dimensional strong-collision-in-J model of Smith and Gilbert (*Int. J. Chem. Kinet.* **1988**, *20*, 307−329) in which ϵ, the energy in the active degrees of freedom, and J, the total angular momentum quantum number, are the independent variables (the ϵ,J model). (3) A two-dimensional variant of the ϵ,J model in which E and J are the independent variables (the E,J model). The third form of the ME is the most physically realistic, and for this model we investigate the dependence of values of the energy transfer moments ($\langle\Delta E_d\rangle$, $-\langle\Delta E\rangle$, and $\langle\Delta E^2\rangle^{1/2}$) deduced from experiment on assumed forms of the energy transfer function, $P(E,E')$, and on temperature. All three moments increase as the temperature rises; $-\langle\Delta E\rangle$ increases from 20−25 cm^{-1} at 300 K to 110−120 cm^{-1} at 4000 K. The variation in the energy transfer moments with the form of $P(E,E')$ depends on the particular moment and the temperature, but generally the variation is not greater than 25%. For the same input to the models, the E and E,J models give similar values of the rate coefficient at high temperature, implying that the rotational degrees of freedom behave increasingly as if they are active as temperature is increased. For $T > 3000$ K, the dissociation perturbs the equilibrium energy distribution of the molecule so much that the detailed-balance condition begins to fail; i.e., $k_0(T)/k_r(T) \neq K_{eq}(T)$, where $k_0(T)$ and $k_r(T)$ are the dissociation and recombination rate coefficients and $K_{eq}(T)$ is the equilibrium constant.

Introduction

Dissociation/recombination reactions play an important role in combustion chemistry. However, predicting (or even estimating) their rate coefficients is ultimately limited by knowledge of collisional energy transfer. The problem is particularly important for small molecules at high temperature (an important regime for combustion), where dissociation (or recombination) occurs at or near the low-pressure limit. Conversely, because low-pressure rate coefficients are so sensitive to collisional energy transfer, they have become an important source of information on quantities such as $\langle\Delta E_d\rangle$ (the average energy transferred in a deactivating collision), $\langle\Delta E\rangle$ (the average energy transferred in all collisions), and $\langle\Delta E^2\rangle^{1/2}$ (the root-mean-squared (RMS) energy transferred in all collisions).[1] This remains the case even though important information about these quantities, as well as information on the energy transfer function itself, $P(E,E')$, can now be obtained from more direct experiments[2−12] and from classical trajectory calculations,[13−24] at least in certain cases.

To extract information about collisional energy transfer from dissociation/recombination rate coefficients, one must solve the master equation (ME). But what constitutes an adequate formulation of the master equation? How sensitive are the calculated results for the rate coefficient to the assumed form of $P(E,E')$? How can one include the effects of molecular rotation in the analysis in a straightforward, yet meaningful, way? The present investigation is an exploratory one in which we seek answers to these questions. We have chosen to limit our discussion to the reaction

$$CH_4 + Ar \rightleftarrows CH_3 + H + Ar$$

because its rate coefficient is known fairly accurately at high temperature,[25−27] and because methane has no properties that are likely to make its dissociation (or the reverse recombination) particularly unusual. Consequently, one might hope that some of our conclusions might be generalizable to other small-molecule dissociations.

In the present work, as part of the analysis, we also derive and discuss a new approximate solution to the two-dimensional master equation in E and J, the total energy and total angular momentum quantum number of the molecule, respectively. This solution is closely related, at least mathematically, to the solution of the 2-D ME of Smith and Gilbert[28] in ϵ and J, where ϵ is the energy in the active degrees of freedom of the dissociating molecule. Both solutions depend on reducing the 2-D ME to an equivalent 1-D equation by making assumptions about the J-dependence of the energy transfer function. The present model appears to capture most of the two-dimensional effects important in thermal dissociation/recombination reactions without introducing the complexity of solving a full two-dimensional master equation.[29−33]

Theory

The Master Equation. In the present investigation we solve three forms of the master equation for thermal dissociation. The

10.1021/jp0144698 CCC: $22.00
Published on Web 04/23/2002

three differ in the way they treat molecular rotation. In the following we describe the reduction of the two-dimensional master equation in E and J to an equivalent one-dimensional model in E. Then we discuss modifications to this model that result in the other two models used in the analysis.

The *E,J* Model. The two-dimensional master equation for the irreversible dissociation of a molecule immersed in an inert gas is

$$\frac{\mathrm{d}n(E,J,t)}{\mathrm{d}t} = Z\sum_{J'}\int_0^\infty [P(E,J;E',J')\, n(E',J',t) - P(E',J';E,J)\, n(E,J,t)]\, \mathrm{d}E' - k(E,J)\, n(E,J,t) \quad (1)$$

where $\mathrm{n}(E,J,t)\,\mathrm{d}E$ is the number density of molecules with total energy between E and $E + \mathrm{d}E$ and total angular momentum quantum number equal to J; t is the time; Z is the collision rate of the molecule with the bath gas; $k(E,J)$ is the unimolecular (RRKM) rate coefficient; and $P(E,J;E',J')$ is the probability of a molecule with energy between E' and $E' + \mathrm{d}E'$ and with total angular momentum quantum number J' being transferred by collision to a state with energy between E and $E + \mathrm{d}E$ and with total angular momentum quantum number equal to J. Letting $n(E,J,t) = n(t)\, x(E,J,t)$, where $x(E,J,t)$ is the normalized population distribution, the left-hand side of eq 1 becomes

$$\frac{\mathrm{d}n(E,J,t)}{\mathrm{d}t} = x(E,J,t)\frac{\mathrm{d}n(t)}{\mathrm{d}t} + n(t)\frac{\mathrm{d}x(E,J,t)}{\mathrm{d}t} \quad (2)$$

If we consider only the regime where the thermal rate coefficient is well defined, the population distribution is in steady state, i.e., $\mathrm{d}x(E,J,t)/\mathrm{d}t = 0$, and $\mathrm{d}n(t)/\mathrm{d}t = -k(T,p)\, n(t)$. Using these results in eq 1 and simplifying, one obtains

$$-k(T,p)\, x(E,J) = Z\sum_{J'}\int_0^\infty P(E,J;E',J')\, x(E',J')\, \mathrm{d}E' - \mathrm{Z}x(E,J) - k(E,J)\, x(E,J) \quad (3)$$

By assuming that $P(E,J;E'J')$ can be written as $P(E,E')\,\varphi(E,J)$ (i.e., the J. distribution after the collision is independent of the angular momentum of the molecule before collision), one can derive from eq 3 an equivalent 1-D model that is analogous to that derived by Smith and Gilbert[28] in the ϵ,J formulation of the master equation. In the present model we assume that $\varphi(E,J)$ is given by

$$\varphi(E,J) = (2J+1)\rho(E,J)/\rho(E) \quad (4)$$

and

$$\rho(E) = \sum_J (2J+1)\rho(E,J) \quad (5)$$

where $\rho(E,J)$ is the density of states of the molecule at energy E and angular momentum quantum number J. Equations 4 and 5 imply that rotational energy is transferred just like vibrational energy and that the J distribution after the collision is simply proportional to the volume of phase space available at any E,J combination. This approximation appears to be reasonably consistent with results from classical trajectory calculations[13−15] in that a collision usually results in comparable quantities of vibrational and rotational energy being transferred.

Using the approximation above in eq 3, one obtains

$$-k(T,p)\, x(E,J) = \mathrm{Z}\varphi(E,J)\sum_{J'}\int_0^\infty P(E,E')\, x(E',J')\, \mathrm{d}E' - \mathrm{Z}x(E,J) - k(E,J)\, x(E,J) \quad (6)$$

Summing over J and defining $\bar{x}(E)$ and $\bar{k}(E)$ as

$$\bar{x}(E) = \sum_J x(E,J) \quad (7)$$

and

$$\bar{k}(E) = \frac{\sum_J k(E,J)\, x(E,J)}{\bar{x}(E)} \quad (8)$$

eq 6 becomes

$$-k(T,p)\,\bar{x}(E) = Z\int_0^\infty P(E,E')\,\bar{x}(E')\,\mathrm{d}E' - Z\bar{x}(E) - \bar{k}(E)\bar{x}(E) \quad (9)$$

Equation 9 has the same form as a one-dimensional master equation in the total energy E, except that calculating $\bar{k}(E)$ requires the solution of the full two-dimensional master equation.[28] To eliminate this problem, we follow the lead of Smith and Gilbert.

Solving eq 6 for $x(E,J)$, we get

$$x(E,J) = \frac{\mathrm{Z}\varphi(E,J)}{Z + k(E,J) - k(T,p)}\int_0^\infty P(E,E')\,\bar{x}(E')\,\mathrm{d}E' \quad (10)$$

Using eq 10 and simplifying, $\bar{k}(E)$ can be written as

$$\bar{k}(E) = \frac{\sum_J k(E,J)\, y(E,J)}{\sum_J y(E,J)} \quad (11)$$

where

$$y(E,J) = \frac{\varphi(E,J)}{Z + k(E,J) - k(T,p)} \quad (12)$$

The form of $\bar{k}(E)$ given by eq 11 highlights the fact that the only dependence of $\bar{k}(E)$ on the solution to the master equation is through $k(T,p)$ in the denominator of $y(E,J)$. As noted by Smith and Gilbert, it is normally a good approximation to take

$$k(T,p) \ll Z + k(E,J) \quad (13)$$

This approximation decouples the calculation of $\bar{k}(E)$ from the solution of eq 9, the desired result. An alternative to making the assumption (13) is to develop an iteration scheme for solving eqs 9 and 11 simultaneously, but this does not appear to be necessary.

The *E* Model. The most direct way of deriving this model is to start with the E,J model and to make the further assumption that

$$x(E,J) = x(E)\,\varphi(E,J) \quad (14)$$

i.e., the J distribution of the population at any E is proportional to the available phase space at that E and J. Then $\bar{x}(E)$ becomes $x(E)$, and using the RRKM expression for $k(E,J)$,

$$k(E,J) = \frac{N^{\pm}(E,J)}{h\rho(E,J)} \quad (15)$$

where h is Planck's constant and $N^{\pm}(E,J)$ is the sum of states at the transition state with energy less than or equal to E and

angular momentum quantum number equal to J, $\bar{k}(E)$ can be written as

$$\bar{k}(E) = \frac{1}{h}\frac{\sum_J (2J+1)N^{\pm}(E,J)}{\rho(E)} \tag{16}$$

If (and only if) there is a single transition state for all J, eq 16 becomes

$$\bar{k}(E) = \frac{1}{h}\frac{N^{\pm}(E)}{\rho(E)} \tag{17}$$

where $N^{\pm}(E)$ is the sum of states (vibrational and rotational) for that transition state with energy less than or equal to E. Note that, in either eq 16 or eq 17, the threshold energy for reaction (i.e., the lowest energy for which $\bar{k}(E) \neq 0$) necessarily corresponds to $J = 0$, because conservation of angular momentum in a rotating molecule always ties up some energy that cannot be used for dissociation. Consequently, in this model, it does not matter whether we resolve the J dependence of the rate constants correctly in the low pressure limit, where only the threshold energies are of concern. However, this is not the case at higher pressures.

Because the threshold energy corresponds to that for $J = 0$, no matter how much energy we put in rotation, and because the sums and densities of states include all the rotational degrees of freedom, this model is completely equivalent to assuming that all rotational degrees of freedom are "active". This statement is true whether or not the reaction is in the low-pressure limit.

The ϵ,J Model. This model is a slightly more general version of that described by Smith and Gilbert. It is what they call a strong-collision-in-J model. First, define the energy in the active degrees of freedom of the molecule to be

$$\epsilon = E - BJ(J+1) \tag{18}$$

where B is the appropriate rotational constant of the molecule. In the present case, because methane is a spherical top, ϵ is the vibrational energy, and the energy in the inactive degrees of freedom is the rotational energy. Stated more succinctly, there are no active rotational degrees of freedom in methane. One can then write a master equation, with ϵ and J as the independent variables, that is identical in form to eq 1. Making the assumption that

$$P(\epsilon,J;\epsilon',J') = P(\epsilon,\epsilon')\,\Phi(\epsilon,J) \tag{19}$$

results in the same simplifications that were obtained above in the E,J model. Taking $\Phi(\epsilon,J)$ to be

$$\Phi(\epsilon,J) = (2J+1)\rho(\epsilon,J)e^{-\beta E_J}/\sum_J (2J+1)\rho(\epsilon,J)e^{-\beta E_J} \tag{20a}$$

where $E_J = BJ(J+1)$, $\beta = (k_B T)^{-1}$, k_B is Boltzmann's constant, and $\rho(\epsilon,J)$ is the density of states of the inactive degrees of freedom with angular momentum quantum number J, results in "strong collisions in J". This model assumes that the post-collision J distribution is thermally equilibrated at the bath gas temperature, independent of ϵ' or J'. Clearly, in both the E,J and ϵ,J models, one could use different forms for $\varphi(E,J)$ and $\Phi(\epsilon,J)$and get different results. However, in both cases the distributions assumed appear to be the only ones that are consistent with detailed balance; i.e., they lead to rotational equilibrium at very long times.

It is worthwhile to comment about the density of states $\rho(\epsilon,J)$ used in eq 20a. In general, $\rho(\epsilon,J)$ has the form

$$\rho(\epsilon,J) = \sum_{\tau=1}^{2J+1} \rho_{vib}(\epsilon - (E_{\tau J} - BJ(J+1)))$$

where $E_{\tau J}$ is the τth eigenvalue of the rotational Hamiltonian for angular momentum quantum number equal to J, and ρ_{vib} is the vibrational density of states. For a symmetric top, one can replace the sum over τ by a sum over the "K" quantum number. For a spherical top such as methane, $E_{\tau J} = BJ(J+1)$ for all τ. Consequently,

$$\rho(\epsilon,J) = (2J+1)\rho_{vib}(\epsilon)$$

and $\Phi(\epsilon,J)$ assumes the particularly simple form

$$\Phi(\epsilon,J) = \frac{(2J+1)^2 e^{-\beta E_J}}{\sum_J (2J+1)^2 e^{-\beta E_J}} \tag{20b}$$

The density of states $\rho(\epsilon)$, used in the detailed balance equation to determine the activating wing of $P(E,E')$from the deactivating wing, is

$$\rho(\epsilon) = \sum_J (2J+1)\rho(\epsilon,J)e^{-\beta E_J}/\sum_J (2J+1)e^{-\beta E_J}$$

The Energy Transfer Function $P(E,E')$. In the present work we investigate the effects of three different forms of the energy transfer function. In all cases a functional form is assumed for the deactivating collisions, i.e., for $E \leq E'$, and the activating wing of $P(E,E')$ is determined from detailed balance. The functional forms used are the following:

exponential

$$P(E,E') = \frac{1}{C_N(E')}\exp(-\Delta E/\alpha), \qquad E \leq E' \tag{21}$$

Gaussian

$$P(E,E') = \frac{1}{C_N(E')}\exp[-(\Delta E/\alpha)^2], \qquad E \leq E' \tag{22}$$

double exponential

$$P(E,E') = \frac{1}{C_N(E')}[(1-f)\exp(-\Delta E/\alpha_1) + f\exp(-\Delta E/\alpha_2)], \qquad E \leq E' \tag{23}$$

In these expressions $C_N(E')$ is a normalization constant, $\Delta E = E' - E$, and the α's and f are parameters in the model. We are interested in three different moments of $P(E,E')$, all evaluated at $E' = E_0$, the dissociation threshold energy:

$$\langle \Delta E \rangle = \int_0^\infty (E - E')P(E,E')\,dE \tag{24}$$

$$\langle \Delta E^2 \rangle = \int_0^\infty (E - E')^2 P(E,E')\,dE \tag{25}$$

$$\langle \Delta E_d \rangle = \int_0^{E'} (E' - E)P(E,E')\,dE / \int_0^{E'} P(E,E')\,dE \tag{26}$$

For the ϵ,J model the same functional forms of $P(\epsilon,\epsilon')$ and the same moments, $\langle \Delta\epsilon_d \rangle$, $\langle \Delta\epsilon \rangle$, and $\langle \Delta\epsilon^2 \rangle$, are of interest. In

practice, we typically adjust the parameters in $P(E,E')$ until we obtain the desired (experimental) rate coefficient from a master equation calculation; then we calculate from eqs 24−26 what that rate constant and energy transfer function imply about the moments of $P(E,E')$.

It is common practice in analyzing thermal dissociation/recombination experiments to assume the exponential-down model for $P(E,E')$ described above. This is at least partially a matter of expedience, since $\alpha \approx \langle \Delta E_d \rangle$ for this model. However, since the classical trajectory analysis of $He-HO_2$ collisional energy transfer by Brown and Miller,[13] virtually all classical trajectory calculations[13−16,18−20,34] and direct experiments[6,12,34] have concluded that the double exponential is a more realistic form for $P(E,E')$. One goal of the present investigation is to quantify the effect of the form of $P(E,E')$ on the values of the moments of ΔE deduced from thermal dissociation experiments. In applying the double-exponential $P(E,E')$, we consider two specific cases: one in which $f = 0.1$ and $\alpha_2 = 10\alpha_1$, and another in which $f = 0.25$ and $\alpha_2 = 5\alpha_1$. The first is crudely based on the trajectory results of Brown and Miller; the second is similarly based on those of Lendvay and Schatz.[16] We call these the 0.1/10 model and the 0.25/5 model, respectively. It should be understood that the two terms in the double exponential function must be of comparable importance in determining $\langle \Delta E_d \rangle$; otherwise the double exponential simply reduces to a single exponential, which could be either the fast or the slow decay, depending on the values of the parameters used in the model. Both terms are important in the two models considered here.

In writing down eq 1 we implicitly assumed that $k(E,J;E',J')$, the rate coefficient for energy transfer, was factorable into a collision rate, $Z(E',J')$, and a probability density function, $P(E,J;E',J')$. We will go even further, as is common practice, and assume that $Z = Z_{LJ}$, where Z_{LJ} is the Lennard-Jones collision rate. All of these assumptions are somewhat questionable.[13−15] However, it should be clear that, if we make it large enough, Z can be taken to be anything as long as $P(E,J;E',J')$ is chosen accordingly. Most experiments are sensitive only to $Z\langle \Delta E \rangle$ (or $Z\langle \Delta E_d \rangle$). Consequently, it is relatively easy to correct for different definitions of Z.

The Lennard-Jones collision rate is probably a reasonable choice for collisions between small molecules and rare-gas atoms in any event. Brown and Miller concluded that, for $He-HO_2$ collisions, $Z(E,J)$ depended weakly on E and J and on average was about 25% larger than Z_{LJ}. Such an error leads to an inconsequential error in $\langle \Delta E \rangle$ or $\langle \Delta E_d \rangle$ in most cases. The majority of subsequent trajectory studies are, more or less, in line with this conclusion.[13,15,21,35] However, Z_{LJ} can be much too small for large molecules, particularly with large-molecule collision partners.[14,15]

Computational Details

All our calculations were carried out with VARIFLEX.[36] The rate coefficients, $k(E,J)$, were calculated from microcanonical, J-resolved, variational transition state theory. A Morse potential was assumed to describe the breaking of the C−H bonds; the transitional degrees of freedom are not important in the low-pressure limit, because the only properties of $k(E,J)$ that play a role in this limit are the J-dependent threshold energies. State counting for methane was done in the harmonic-oscillator/rigid-rotor approximation. Vibrational sums and densities of states were calculated by the method of steepest descent (rather than exact account) in order to avoid oscillations in these quantities as the bin width, δE, was reduced, a desirable property for ensuring accuracy. The two methods of state counting give very similar results anyway. Most of the calculations reported here were done with δE (or $\delta\epsilon$) = 25 cm^{-1}. However, a δE of 10 cm^{-1} was employed in some cases. Such small values of δE were necessary to resolve satisfactorily the fast exponential in the double-exponential energy transfer functions in some cases and even the $\langle \Delta\epsilon_d \rangle$ deduced from the single-exponential function in the ϵ,J model. Numerical values of molecular constants are given in the appendix.

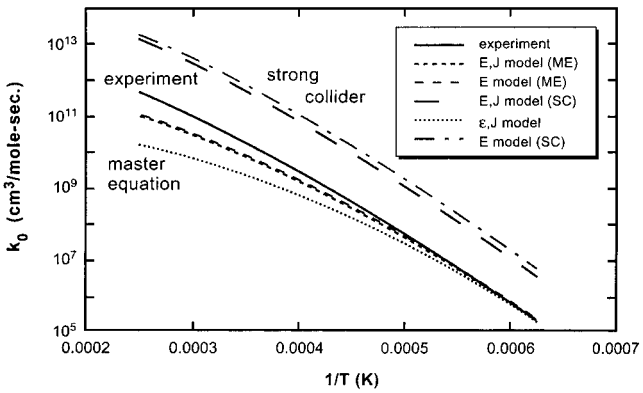

Figure 1. High-temperature rate coefficients. The master-equation calculations were done with $\langle \Delta E_d \rangle = 410$ cm^{-1}, independent of T, for the E,J and E models. A constant value of $\langle \Delta\epsilon_d \rangle = 35$ cm^{-1} was assumed for the ϵ,J ME calculations.

The master equation (eq 9) can be recast in the form

$$G|w\rangle = -k(T,p)|w\rangle \tag{27}$$

where the vector $|w\rangle$ contains the steady-state energy level populations and G is a real, symmetric matrix. Then, $k(T,p)$ can be calculated as $k(T,p) = -\lambda_1$, where λ_1 is algebraically the largest (least negative) eigenvalue of G. We used several methods to calculate λ_1 in order to ensure accuracy under all conditions investigated. Normally we calculated $k(T,p)$ at two different pressures, $p = 10^{-3}$ Torr and $p = 10^{-2}$ Torr, to be certain that $k(T,p)$ was linear in pressure. The low-pressure limit rate coefficient, $k_0(T)$, is easily determined from these results. The low-temperature eigenvalue problem is averted by using the "matrix inversion" technique of Pilling and co-workers,[41] a standard option in VARIFLEX, and assuming that thermal equilibrium is maintained below a specified energy, the value of which is varied with temperature to ensure accuracy.

Results and Discussion

High Temperature. As noted in the Introduction, at high T the low-pressure-limit rate coefficient, $k_0(T)$, for $CH_4 + Ar \rightleftarrows CH_3 + H + Ar$, is relatively well established from shock-tube experiments. Kiefer and Kumaran[25] give the expression

$$\log k_0(\mathrm{cm^3/(mol\ s)}) = 47.279 - 8.106 \log T - 25660/T \tag{28}$$

for the temperature range, 1600 K ≤ T ≤ 4000 K, accurate to ±50%. We take this to be the correct result with the understanding that there is a small degree of uncertainty in the rate coefficient.

In Figure 1 we have plotted the expression above on an Arrhenius plot, along with the strong-collider results from the E,J and E models and the master equation results from the E,J,

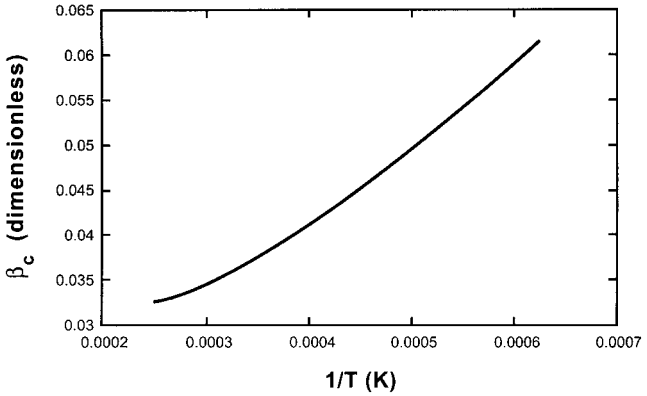

Figure 2. Weak-collision efficiency factor for the Kiefer and Kumaran[25] rate coefficient.

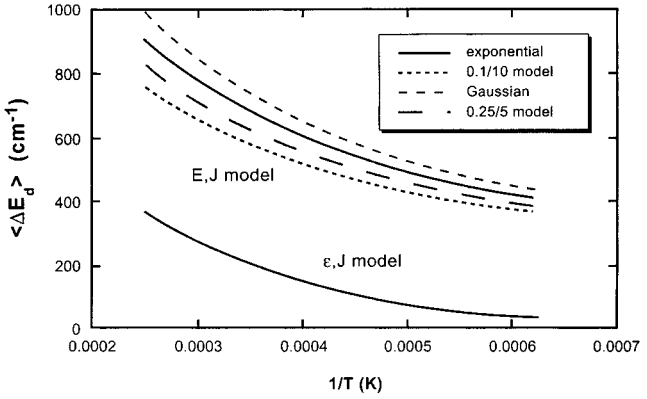

Figure 3. Values of $\langle\Delta E_d\rangle$, or $\langle\Delta\epsilon_d\rangle$, deduced from the Kiefer and Kumaran[25] rate coefficient using the E,J model, or ϵ,J model.

the ϵ,J, and the E models; the exponential-down function was used for $P(E,E')$,or $P(\epsilon,\epsilon')$, in the ME calculations. In these latter calculations, $\langle\Delta E_d\rangle$ was taken to be 410 cm^{-1} in the E and E,J models, and $\langle\Delta\epsilon_d\rangle$ was taken equal to 35 cm^{-1} in the ϵ,J model. These values were deduced from the experimental rate coefficient at 1600 K. For reference, the weak collision efficiency factor, $\beta_c(T) = k_0(T)/k_0^{sc}(T)$, is plotted in Figure 2; it was determined from the experimental $k_0(T)$ and the E,J result for $k_0^{sc}(T)$. The value of β_c drops off rapidly with increasing temperature, approaching the low value of $\beta_c \approx 3 \times 10^{-2}$ at very high temperatures.

From Figure 1 it is clear that taking $\langle\Delta E_d\rangle$ or $\langle\Delta\epsilon_d\rangle$ equal to a constant is not a very good approximation. Assuming the values of these parameters deduced at 1600 K to be valid at 4000 K leads to an error of approximately a factor of 4 for the rate coefficients in the E,J and E models and a factor of 40 in the ϵ,J model. Somewhat surprisingly, the E,J and E models give rate coefficients that are very similar both for the strong-collision limit and in the ME calculations. The two ME results are actually even closer than the two strong-collider rate coefficients. The near equality of the E,J and E rate coefficients implies that the rotational degrees of freedom in methane behave as if they are active at these temperatures. However, as discussed below, this is not the case at lower temperatures.

In Figures 3−5 we have plotted the moments of the energy transfer function versus $1/T$ for the four forms of $P(E,E')$ described above; these were calculated using the E,J master-equation model by forcing very precise agreement between the theoretical $k_0(T)$ and that obtained from eq 28. Also shown in the figures are the moments of $P(\epsilon,\epsilon')$ similarly determined from the ϵ,J model with the exponential-down form for $P(\epsilon,\epsilon')$. The differences in $\langle\Delta E_d\rangle$, $\langle\Delta E\rangle$, and $\langle\Delta E^2\rangle^{1/2}$ obtained using different

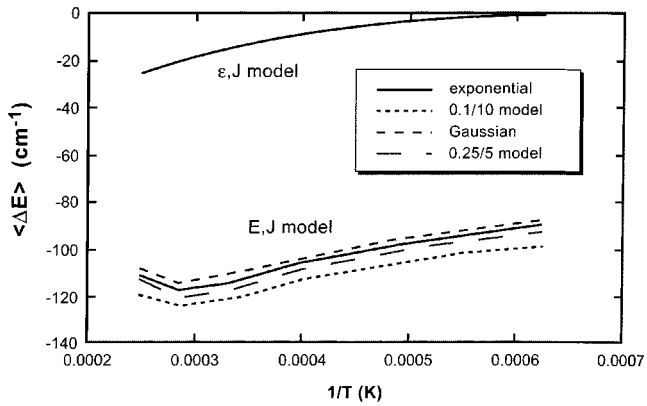

Figure 4. Values of $\langle\Delta E\rangle$, or $\langle\Delta\epsilon\rangle$, deduced from the Kiefer and Kumaran[25] rate coefficient using the E,J model, or ϵ,J model.

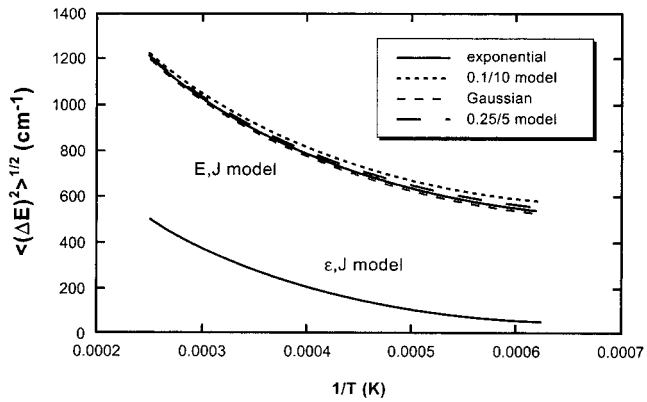

Figure 5. Values of $\langle\Delta E^2\rangle^{1/2}$, or $\langle\Delta\epsilon^2\rangle^{1/2}$, deduced from the Kiefer and Kumaran[25] rate coefficient using the E,J model, or ϵ,J model.

forms of $P(E,E')$ are not large, varying from less than 10% to roughly 25%, depending on the temperature and the particular moment being considered. The biggest difference is for $\langle\Delta E_d\rangle$ at 4000 K, where the 0.1/10 model yields a $\langle\Delta E_d\rangle < 800$ cm^{-1} and the Gaussian function gives $\langle\Delta E_d\rangle \approx 1000$ cm^{-1}. The general trend is that $P(E,E')$ functions with longer tails (the 0.1/10 and 0.25/5 models) give smaller values of $\langle\Delta E_d\rangle$ and larger values of $\langle\Delta E^2\rangle^{1/2}$ and $-\langle\Delta E\rangle$ than do the other functions. As noted several times previously,[37−41] $\langle\Delta E_d\rangle$ (and $\langle\Delta E^2\rangle^{1/2}$) values obtained from thermal dissociation/recombination experiments increase substantially with increased temperature. Conversely, $-\langle\Delta E\rangle$ is a relatively weak function of temperature, increasing slowly from 1600 to 3500 K in the present case, then decreasing slightly between 3500 and 4000 K. The latter effect could simply be an artifact of the experiment. These results indicate that $\langle\Delta E\rangle \approx$ const., independent of temperature, may be a reasonable first approximation in modeling unimolecular reactions when there is no better information available—it is certainly better than taking $\langle\Delta E_d\rangle =$ const.

We calculated the moments of $P(\epsilon,\epsilon')$ from the ϵ,J model only for the exponential-down form of the energy transfer function. The double exponential forms of $P(\epsilon,\epsilon')$, which are of the most interest, would have required a very small bin width $\delta\epsilon$ to resolve satisfactorily the faster decaying exponentials in these functions, at least for values of the moments similar to those obtained for the single exponential. The accompanying expenditure of computer resources for such small $\delta\epsilon$ does not appear to be worth the effort. The values of $\langle\Delta\epsilon_d\rangle$, $-\langle\Delta\epsilon\rangle$, and $\langle\Delta\epsilon^2\rangle^{1/2}$ shown in Figures 3−5 appear to be unrealistically small. At 1600 K, $\langle\Delta\epsilon_d\rangle = 35$ cm^{-1} and $-\langle\Delta\epsilon\rangle = 0.83$ cm^{-1}. Although there are no direct experiments for methane, there is no

evidence to support such small vibrational energy transfer rates either from experiment[6−9] or from trajectory calculations[13,14,16] for molecules of any size. One is forced to conclude that the strong-collision-in-J approximation (eqs 9 and 20) is not an adequate representation of reality, at least in the present case.

The most likely explanation for the failure of the strong-collision-in-J approximation is that it implies that unreasonably large quantities of rotational energy are transferred in a collision for states near the dissociation limit. As noted above, methane at these temperatures behaves as if its rotational degrees of freedom are active. Consequently, if large quantities of rotational energy are transferred in a collision, not much vibrational energy transfer is required to dissociate the molecule.

Kiefer and Kumaran[25] and Cobos and Troe[42,43] have used the Troe factorization scheme[44−46] to extract values of $-\langle\Delta E\rangle$ from the same experiments considered here. They give 112 and 50 ($\pm$20) cm^{-1} for $-\langle\Delta E\rangle$, respectively. Both these results are of the same order of magnitude as those shown in Figure 4. However, it is not obvious that this comparison is valid. The $\langle\Delta E\rangle$ in the Troe factorization method is a rather ill-defined quantity. Troe describes it in the following way:[45] "If coupled vibrational and rotational energy transfer have to be considered, $\langle\Delta E\rangle$ corresponds to a complex average over vibrational and rotational energy transfer weighted by a centrifugal barrier function." For the present high-temperature calculations, where the rotations act like they are active, our definition of $\langle\Delta E\rangle$, the average total energy transferred in a collision, may well be directly comparable to the Troe $\langle\Delta E\rangle$. However, at lower temperatures for the present reaction and for other reactions, such may not be the case.

The discussion of the pervious paragraph points up a problem. There are at least three ways of deducing values of $\langle\Delta E\rangle$ from thermal dissociation experiments that are common in the literature:

(1) The Troe factorization method.

(2) Solution of a one-dimensional master equation in which E, the total energy, is the independent variable. This is necessarily the approach when $k(E)$ is calculated from a $k(T)$ by inverse Laplace transform. This method is equivalent to our E model.

(3) Solution of a one-dimensional master equation in which ϵ, the energy in the active degrees of freedom, is the independent variable. In this case, it is values of $\langle\Delta\epsilon\rangle$ that are deduced, although not necessarily under the same assumption about rotation as our ϵ,J model. It is tempting to compare directly values of $\langle\Delta E\rangle$, or other moments of $P(E,E')$, deduced by these three approaches. However, it is clear that they are not directly comparable, and it is by no means obvious exactly how one is related to the other.

It is common practice to assume that one can calculate the recombination rate coefficient, k_r, from k_0 and the equilibrium constant,

$$\frac{k_0(T)}{k_r(T)} = K_{eq}(T) \tag{29}$$

However, this point was seriously debated in the 1950s and early 1960s when it was first realized that high-temperature dissociation of small molecules necessarily involves nonequilibrium energy distributions of bound states. It was not until 1989 that Smith et al.[47] derived a rigorous condition for the validity of eq 29. Although their result is not limited to the low-pressure limit, in the present context, Smith et al. showed that

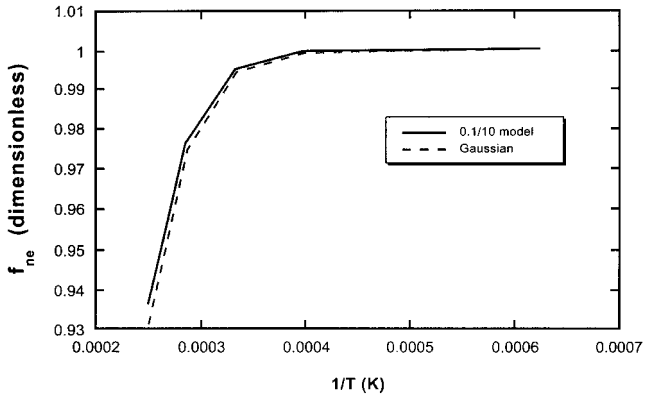

Figure 6. Nonequilibrium factor, defined by eq 31, as a function of temperature.

$$\frac{k_0(T)}{k_r(T)} = \frac{1}{f_{ne}(T)} K_{eq}(T) \tag{30}$$

where

$$f_{ne}(T) = \frac{\left(\int_0^\infty dE\, \bar{x}(E)\right)^2}{\int_0^\infty dE\, \dfrac{\bar{x}^2(E)}{f(E)}} \tag{31}$$

$$f(E) = \rho(E) e^{-\beta E}/Q(T) \tag{32}$$

and $Q(T)$ is the vibrational−rotational partition function of the dissociating molecule. It is rare for $f_{ne}(T)$ to deviate significantly from unity, so that typically eq 29 is satisfied to a high degree of accuracy. However, because of the very high temperatures involved, it is instructive to investigate the applicability of eq 29 in the Kiefer and Kumaran experiments.

Values of $f_{ne}(T)$ calculated from the E,J master equation using the 0.1/10 and Gaussian energy transfer models (the others are intermediate in value) are plotted in Figure 6. Up to $T = 3000$ K, $f_{ne} \approx 1$. In fact, for $T = 2000$ K and below, $f_{ne} = 1.0000$; i.e., there are at least four zeros after the decimal point. However, for $T > 3000$ K, $f_{ne}(T)$ begins to deviate significantly from unity. In fact, if we were interested in methane dissociation at 5000 K, the applicability of eq 29 would be seriously in question.

Let us look at what happens in the present case to the steady-state populations, $\bar{x}(E)$ as temperature increases. The ratio $\bar{x}(E)/f(E)$, at various temperatures is plotted in Figure 7 for both the E,J (Figure 7a) and E (Figure 7b) master equation models using the exponential-down form of $P(E,E')$ with the $\langle\Delta E_d\rangle$ values deduced from the experiments. The depletion of $\bar{x}(E)$ below $f(E)$ for bound states near the dissociation limit is well-known to be the reason $\beta_c \neq 1$ at high temperature and why β_c gets increasingly smaller as temperature increases. However, it is not commonly appreciated that overpopulation (i.e., $\bar{x}(E)/f(E) > 1$) of states at lower energies is the cause of the breakdown of eq 29 at high T.

From eq 31, because $\bar{x}(E)$ and $f(E)$ are normalized to unity, it can be seen that $f_{ne}(T) = 1$ as long as $\bar{x}(E) = f(E)$ for all states that are substantially populated in steady state. To make

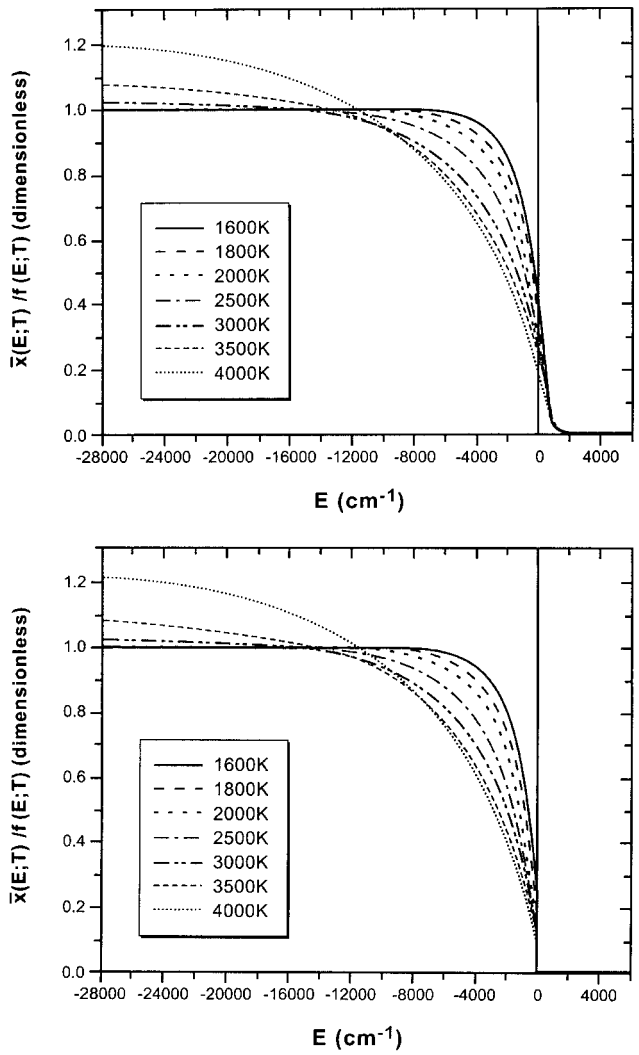

Figure 7. $\bar{x}(E;T)/f(E;T)$ for various temperatures. The zero of energy is the threshold energy E_0. (a) *E,J* model. (b) *E* model. The calculations were done with the exponential-down form of $P(E,E')$ and $\langle \Delta E_d \rangle$ values from Figure 3.

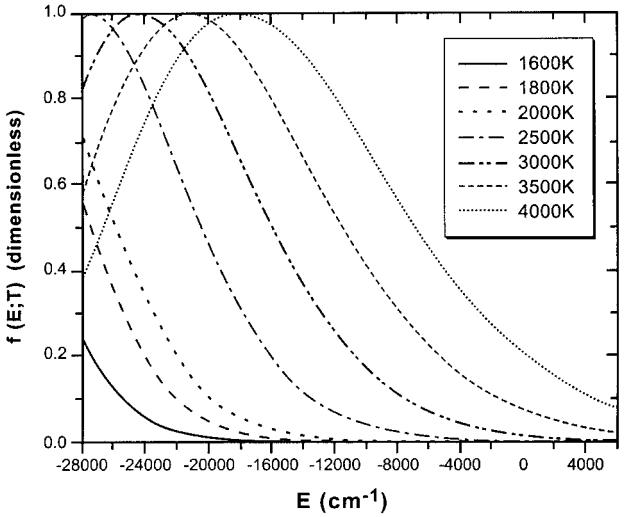

Figure 8. Relative values of $f(E;T)$. The functions are normalized so that the peak is always unity.

this point clearer, one can write $f_{ne}(T)$ as

$$f_{ne}(T) = \frac{1}{\int_0^\infty dE \, \frac{\bar{x}(E)}{f(E)} \bar{x}(E)} \tag{33}$$

If $\bar{x}(E) = f(E)$, $f_{ne}(T) \rightarrow 1$. The only way that $f_{ne}(T)$ can be less than unity, as is the case in Figure 6, is if $\bar{x}(E)/f(E)$ is greater than unity for states that have significant population at steady state. Comparing Figure 7 with Figure 8, which is a plot of relative $f(E)$ values at various temperatures, one can see that the situation just described begins to occur at $T \approx 3000$ K, just as $f_{ne}(T)$ begins to drop off in Figure 6. Consequently, one can conclude that eq 29 fails at high temperature because of a complicated perturbation of the equilibrium distribution (overpopulation at low energies necessitated by depletion at high energies) caused by the dissociation process. A cursory examination of other eigenvectors of G under these conditions indicates that this perturbation is accompanied by small contributions to the dissociation from some of the energy relaxation eigenvectors; these contributions ultimately cause the failure of the rate constant approximation at sufficiently high temperature.

One is tempted to conclude that deviations of f_{ne} from unity are not of practical importance, because they are limited to such high temperature. However, for molecules larger than methane that also have weaker bonds, f_{ne} will begin to deviate from unity at much lower temperatures, perhaps in the 1000−2000 K temperature range that is most important for combustion applications.

Another important feature of the two-dimensional master-equation calculations is shown in Figure 7. In the *E,J* model there is significant population at steady state above the dissociation threshold ($E = 0$ in the figure), whereas there is none in the *E* model. Because of angular momentum conservation, high *J* states require more total energy to produce dissociation than do lower ones. Of course, this property is missing in the *E* model where all *J* states are assumed to have the same threshold energy. Consequently, the *E* model tends to produce larger rate constants than the *E,J* model. However, there is a compensating effect. Because the dissociation threshold is actually "closer" to these states in the *E* model than in the *E,J* model, populations of bound states with high *J* have lower steady-state populations in the *E* model than they do in the *E,J* model. This effect reduces the rate constants from the *E* model relative to those from the *E,J* model. It is the reason the difference between the two models is greater for the strong-collider rate constants in Figure 1 than for the master-equation results.

Low Temperature. Unlike the situation at high temperature, the low-temperature rate coefficient is not well established. Of course, at low temperatures we are interested in the low-pressure limit of the recombination reaction,

$$CH_3 + H + Ar \rightleftarrows CH_4 + Ar$$

whose rate coefficient is related to the dissociation rate coefficient $k_0(T)$ by eq 29, at least up to a temperature of about 3000 K. For the purposes of analysis, we take the CEC recommendation[48] to be the correct value of k_r even though it is apparent from our analysis that this is probably not the case, at least at the upper end of the suggested temperature range, 300 K < T < 1000 K. The rate coefficient $k_r(T)$ (low-pressure limit) is given in the CEC review as

$$k_r = 6.26 \times 10^{23} \, T^{-1.8} \text{cm}^6/(\text{mol}^2 \, \text{s}) \tag{34}$$

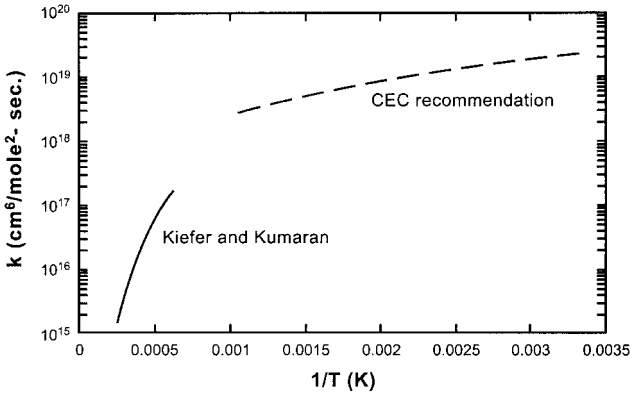

Figure 9. Recombination rate coefficient.

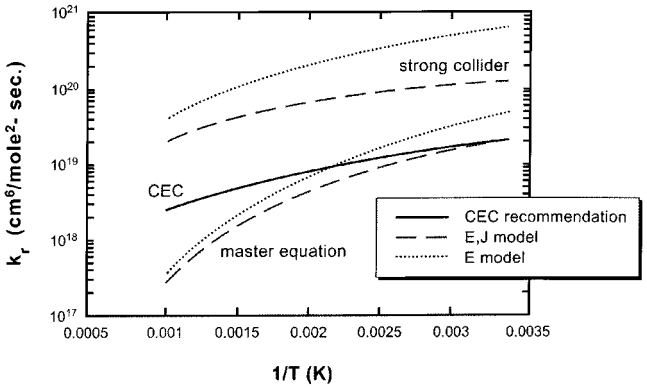

Figure 10. Low-temperature recombination rate coefficients. The master-equation calculations were done with the exponential-down form of $P(E,E')$ and with $\langle\Delta E_d\rangle = 80$ cm^{-1}.

This expression is plotted in Figure 9 with the recombination rate coefficient obtained from the Kiefer and Kumaran result for $k_0(T)$ and the equilibrium constant. It is clear from this plot that the CEC expression does not blend smoothly with the shock tube results. Nevertheless, at least the rate coefficients up to $T \approx 800$ K appear to be a reasonable extrapolation of the Kiefer and Kumaran expression. The inconsistency of the two rate expressions is even more apparent in some of the results presented below.

Figure 10 is a plot of the CEC rate constant, the strong-collider predictions from both the *E,J* and *E* models, and the ME results from the two models using the exponential-down energy transfer function with a value of $\langle\Delta E_d\rangle = 80$ cm^{-1}. This value of $\langle\Delta E_d\rangle$ was deduced from the CEC rate constant at 300 K using the *E,J* master equation formulation. Because of the small values of $\langle\Delta\epsilon_d\rangle$ (and $-\langle\Delta\epsilon\rangle$) implied by the ϵ,*J* ME formulation, a prohibitively small value of $\delta\epsilon$ is required for these calculations, as discussed above. However, calculations at $T = 300$ K with $\delta\epsilon = 10$ cm^{-1} resulted in $\langle\Delta\epsilon_d\rangle < 5$ cm^{-1} and $-\langle\Delta\epsilon\rangle < 0.3$ cm^{-1} necessary to obtain the CEC rate constant at that temperature. For the same reason as discussed above, such values appear to be unrealistically small.

Unlike the high-temperature calculations, Figure 10 shows significant differences between the *E,J* and *E* models at low temperature, both for the ME calculations and in the strong-collider limit. At 300 K, the ratio of the *E*-model rate coefficient to that for the *E,J* model is 5.15 in the strong-collider limit and 2.23 for the master-equation results. The two ratios drop to 2.04 and 1.27, respectively, at 1000 K. As the temperature increases, the CH_4 dissociation/recombination behaves more and more like the rotational degrees of freedom are active. At temperatures above 1600 K, as shown in Figure 1, this becomes a good approximation.

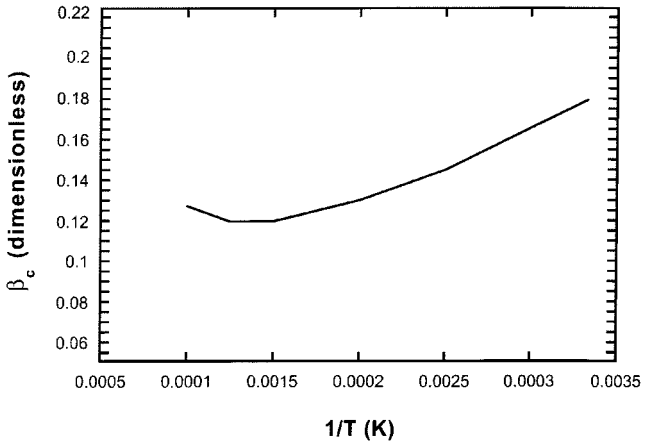

Figure 11. Weak-collision efficiency factor from the CEC rate coefficient.

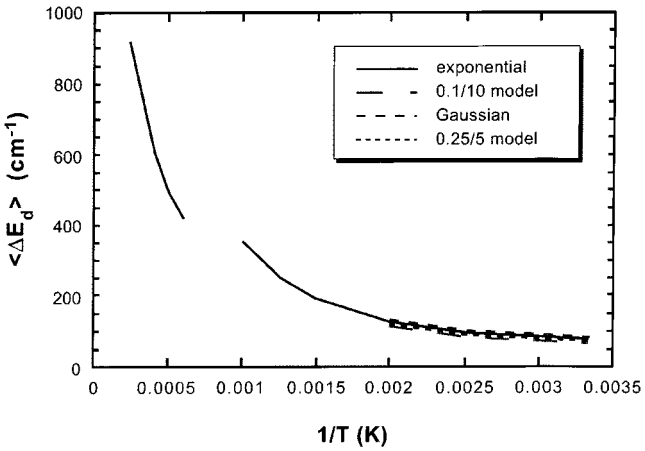

Figure 12. Values of $\langle\Delta E_d\rangle$ deduced from the *E,J* model.

Figure 10 also shows that $\langle\Delta E_d\rangle$ = const. is not a good approximation at low *T*, as was also the case at high temperature. The error incurred by assuming $\langle\Delta E_d\rangle = 80$ cm^{-1}, independent of temperature, is approximately a factor of 9.5 at 1000 K if the CEC rate coefficient is assumed to be correct. However, another indication that the CEC recommendation is not accurate at the high end of the temperature range is shown in Figure 11, which is a plot of $\beta_c(T)$ (based on the CEC rate coefficient and the *E,J* strong-collider result) as a function of temperature. For $T > 800$ K, $\beta_c(T)$ actually increases with temperature, an extremely unlikely result.

Figures 12−14 show values of $\langle\Delta E_d\rangle$, $-\langle\Delta E\rangle$, and $\langle\Delta E^2\rangle^{1/2}$ as a function of *T* deduced from the CEC rate coefficients using the four different forms of $P(E,E')$. These results show trends similar to those deduced from the Kiefer and Kumaran rate coefficient at high temperature; i.e., $\langle\Delta E_d\rangle$, $-\langle\Delta E\rangle$, and $\langle\Delta E^2\rangle^{1/2}$ all increase with temperature. Viewed as a whole (keeping in mind the potential errors in the CEC rate coefficient), it seems fair to conclude from these results that $\langle\Delta E_d\rangle$ and $\langle\Delta E^2\rangle^{1/2}$ increase relatively slowly with temperature from $T = 300$ K up to perhaps 1000 K, then much more rapidly beyond 1000 K. Values of $-\langle\Delta E\rangle$ also rise with temperature from $-\langle\Delta E\rangle \approx 20-25$ cm^{-1} at 300 K to $-\langle\Delta E\rangle \approx 110-120$ cm^{-1} at 4000 K. In contrast to the high-temperature results, $\langle\Delta E_d\rangle$ depends very weakly on the form of $P(E,E')$ at low *T*. The form of the energy transfer function has relatively little effect on $-\langle\Delta E\rangle$ and $\langle\Delta E^2\rangle^{1/2}$ at either low or high temperature.

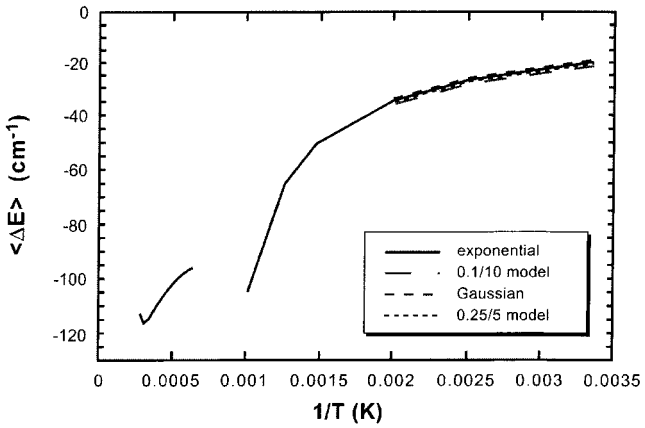

Figure 13. Values of $\langle \Delta E \rangle$ deduced from the *E*,*J* model.

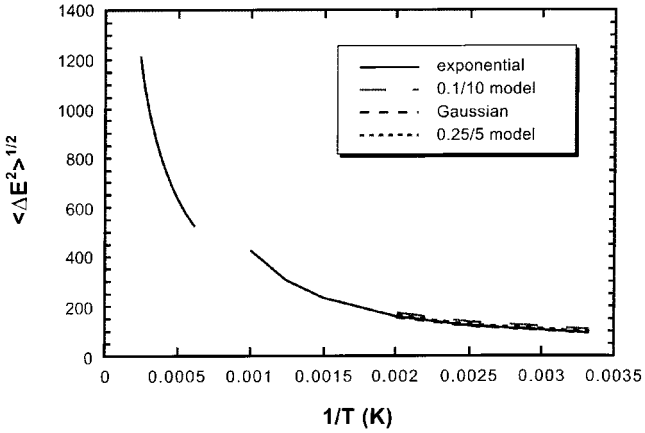

Figure 14. Values of $\langle \Delta E^2 \rangle^{1/2}$ deduced from the *E*,*J* model.

Concluding Remarks

We have studied the dissociation of methane in the low-pressure limit using three forms of the master equation: the *E* formulation, the *E*,*J* formulation, and the ϵ,*J* formulation. In the *E*,*J* model, the best of the three formulations, we employed four different energy transfer functions to deduce values of $\langle \Delta E_d \rangle$, $\langle \Delta E \rangle$, and $\langle \Delta E^2 \rangle^{1/2}$ from experimental rate coefficients. As temperature increases from 300 to 4000 K, $\langle \Delta E_d \rangle$, $-\langle \Delta E \rangle$, and $\langle \Delta E^2 \rangle^{1/2}$ all increase continuously. The values of $\langle \Delta E_d \rangle$ and $\langle \Delta E^2 \rangle^{1/2}$ increase relatively slowly from 300 K up to perhaps 1000 K, then more rapidly between 1000 and 4000 K; $-\Delta E$ increases from 20−25 cm^{-1} at 300 K to approximately 110−120 cm^{-1} at 4000 K. These trends are generally independent of the form of $P(E,E')$. The dependence of $\langle \Delta E_d \rangle$ on $P(E,E')$ is greatest at high temperature, whereas the variation in $\langle \Delta E^2 \rangle^{1/2}$ with $P(E,E')$ is relatively small at all temperatures. The spread in $-\langle \Delta E \rangle$ values with $P(E,E')$ increases slightly from only about 3 cm^{-1} at 300 K to approximately 10 cm^{-1} at 4000 K.

The ϵ,*J* model (i.e., the strong-collision-in-*J* approximation[28]) yields unreasonably small values of $\langle \Delta \epsilon_d \rangle$, $\langle \Delta \epsilon^2 \rangle^{1/2}$, and $-\langle \Delta \epsilon \rangle$, probably because it implies that excessively large quantities of rotational energy are transferred in a collision for states near the dissociation limit. If everything else in the theory is kept the same, the *E* and *E*,*J* models give significantly different rate coefficients at low temperature, but this difference disappears as temperature is increased. This latter result implies that the rotational degrees of freedom behave more and more as if they are active as the temperature rises.

For $T > 3000$ K, the relationship $k_0/k_r = K_{eq}$ begins to fail. This failure occurs because of a complicated perturbation of the equilibrium energy distribution caused by the dissociation process. The most important aspect of this perturbation is that states that are heavily populated at equilibrium are overpopulated by the perturbation.

Acknowledgment. This work was supported by the United States Department of Energy, Office of Basic Energy Sciences, Division of Chemical Sciences, Geosciences and Biosciences.

Appendix

Methane

Vibrational frequencies (cm^{-1}) with degeneracies
3019(3), 2917, 1534(2), 1306(3)
rotational constant (cm^{-1})
5.31
threshold energy, E_0 (kcal/mol)
103.34
Lennard-Jones parameters
$\sigma = 3.33$ Å
$\epsilon = 94.9$ cm^{-1}

Argon

Lennard-Jones parameters
$\sigma = 3.75$ Å
$\epsilon = 98.3$ cm^{-1}

References and Notes

(1) Tsang, W.; Kiefer, J. H. In *Chemical Dynamics and Kinetics of Small Radicals*; Wager, A. F., Lui, K., Eds.; World Scientific: Singapore, 1995; Part I, pp 58−119.
(2) Barker, J. R.; Yoder, L. M.; King, K. D. *J. Phys. Chem. A* **2001**, *103*, 796−809.
(3) Brenner, J. D.; Erinjeri, J. P.; Barker, J. P. *Chem. Phys*. **1993**, *175*, 99−111.
(4) Mullin, A. S.; Park, J.; Chou, J. Z.; Flynn, G. W.; Weston, R. E. *J. Chem. Phys*. **1993**, *53*, 175.
(5) Mullin, A. S.; Michaels, C. A.; Flynn, G. W. *J. Chem. Phys*. **1995**, *102*, 6032.
(6) Michaels, C. A.; Flynn, G. W. *J. Chem. Phys*. **1997**, *106*, 3558−3566.
(7) Grigoleit, U.; Lenzer, T.; Luther, K.; Mützel, M.; Takahara, A. *Phys. Chem. Chem. Phys*. **2001**, *3*, 2192−2202.
(8) Lenzer, T.; Luther, K.; Reihs, K.; Symonds, A. C. *J. Chem. Phys.* **2000**, *112*, 4090−4110.
(9) Hold, U.; Lenzer, T.; Luther, K.; Reihs, K.; Symonds, A. C. *J. Chem. Phys*. **2000**, *112*, 4076−4089.
(10) Luther, K.; Reihs, K. *Ber. Bunsen-Ges. Phys. Chem*. **1988**, *92*, 442.
(11) Löhmannsröben, H. G.; Luther, K. *Chem. Phys. Lett.* **1988**, *144*, 473.
(12) Hold, U.; Lenzer, T.; Luther, K.; Reihs, K.; Symonds, A. C. *Ber. Bunsen-Ges. Phys. Chem*. **1997**, *101*, 552−565. Troe, J. *J. Chem. Phys.* **1977**, *66*, 4758−4775.
(13) Brown, N. J.; Miller, J. A. *J. Chem. Phys.* **1984**, *80*, 5568.
(14) Lendvay, G.; Schatz, G. C. Classical Trajectory Methods for Studying Energy Transfer from Highly Vibrationally Excited Molecules. In *Vibrational Energy Transfer in Large and Small Molecules*; Barker, J. R., Ed.; JAI Press: Greenwich, CT, 1995; Vol. 2.B, pp 481−513.
(15) Nordholm, S.; Schranz, H. W. Collisional Energy Transfer in Unimolecular Reactions: Statistical Theory and Classical Simulation. In *Vibrational Energy Transfer in Large and Small Molecules*, Barker, J. R., Ed.; JAI Press: Greenwich, CT, 1995; Vol. 2.A, pp 245−281.
(16) Lendvay, G.; Schatz, G. C. *J. Phys. Chem*. **1994**, *98*, 6530−6536.
(17) Oref, I. Supercollisions. In *Vibrational Energy Transfer in Large and Small Molecules*, Barker, J. R., Ed.; JAI Press: Greenwich, CT, 1995; Vol. 2B, pp 285−298.
(18) Higgins, C.; Ju, Q.; Seiser, N.; Flynn, G. W.; Chapman, S. *J. Phys. Chem A* **2001**, *105*, 2858−2866.
(19) Lenzer, T.; Luther, K., Troe, J.; Gilbert, R. G.; Lim, K. F. *J. Chem. Phys.* **1995**, *103*, 626−641.
(20) Bernshtein, V.; Oref, I.; Lendvay, G. *J. Phys. Chem.* **1996**, *100*, 9738−9744.
(21) Gilbert, R. G. *Int. Rev. Phys. Chem.* **1991**, *10*, 319−347.
(22) Clarke, D. L.; Thompson, K. C.; Gilbert, R. G. *Chem. Phys. Lett.* **1991**, *182*, 357−362.
(23) Grigoleit, U.; Lenzer, T.; Luther, K. *Z Phys. Chem.* **2000**, *213*, 1065−1085.
(24) Bernstein, V.; Oref, I. *J. Chem. Phys.* **1998**, *108*, 3543−3553.

(25) Kiefer, J. H.; Kumaran, S. S. *J. Phys. Chem.* **1993**, *97*, 414−420.
(26) Davidson, D. F.; DiRosa, M. D.; Chang, A. Y.; Hanson, R. K.; Bowman, C. T. *Proc. Combust. Inst.* **1992**, *24*, 589−596.
(27) Sutherland, J. W.; Su, M.-C.; Michael, J. V. *Int. J. Chem. Kinet*. **2001**, *33*, 669−684.
(28) Smith, S. C.; Gilbert, R. G. *Int. J. Chem. Kinet*. **1988**, *20*, 307−329.
(29) Jeffrey, S. J.; Gates, K. E.; Smith, S. C. *J. Phys. Chem.* **1996**, *100*, 7090−7096.
(30) Robertson, S. H.; Pilling, M. J.; Green, N. J. B. *Mol. Phys.* **1996**, *89*, 1531.
(31) Robertson, S. H.; Pilling, M. J.; Gates, K. E.; Smith, S. C. *J. Chem. Phys.* **1997**, *18*, 1004−1010.
(32) Robertson, S. H.; Shushin, A. I.; Wardlaw, D. M. *J. Chem. Phys.* **1993**, *98*, 8673−8679.
(33) Smith, S. C.; McEwan, M. J.; Gilbert, R. J. *J. Chem. Phys.* **1989**, *90*, 1630−1640.
(34) Troe, J. *J. Chem. Phys*. **1992**, *97*, 288−292.
(35) Troe, J. *J. Phys. Chem.* **1979**, *83*, 114−126.
(36) Klippenstein, S. J.; Wagner, A. F.; Dunbar, R. C.; Wardlaw, D. M.; Robertson, S. H.; Miller, J. A. Variflex: Version 1.10m, 2001.
(37) Knyazev, V. D.; Slagle, I. R. *J. Phys. Chem.* **1996**, *100*, 16899−16911.
(38) Feng, Y.; Nüranen, J. T.; Benesura, A.; Knyazev, V. D.; Gutman, D.; Tsang, W. *J. Phys. Chem.* **1993**, *97*, 871−880.
(39) Knyazev, V. D.; Tsang, W. *J. Phys. Chem. A* **2000**, *104*, 10747−10765.
(40) Knyazev, V. D.; Dubinsky, I. A.; Slagle, I. R.; Gutman, D. *J. Phys. Chem.* **1994**, *98*, 5279−5289.
(41) Hanning-Lee, M. A.; Green, N. J. B.; Pilling, M. J.; Robertson, S. H. *J. Phys. Chem.* **1993**, *97*, 860−870.
(42) Cobos, C. J.; Troe, J. *Z. Phys. Chem*. **1992**, *176*, 161−171.
(43) Cobos, C. J.; Troe, J. *Z. Phys. Chem. Neue Folge* **1990**, *167*, 129.
(44) Troe, J. *J. Phys. Chem.* **1977**, *66*, 4758−4775.
(45) Troe, J. *J. Chem. Phys.* **1977**, *66*, 4745−4757.
(46) Gilbert, R. G.; Luther, K.; Troe, J. *Ber. Bunsen-Ges. Phys. Chem.* **1983**, *87*, 169−177.
(47) Smith, S. C.; McEwan, M. J.; Gilbert, R. J. *J. Chem. Phys.* **1989**, *90*, 4265−4273.
(48) Baulch, D. L.; Cobos, C. J.; Cox, R. A.; Frank, P.; Hayman, G.; Just, Th.; Kerr, J. A.; Murrells, T.; Pilling, M. J.; Troe, J.; Walker, R.; Warnatz, J. *J. Phys. Chem. Ref. Data* **1994**, *23*, 847−1033.